Performance of Cavity-Parametric Amplifiers, Employing Kerr Nonlinearites, in the Presence of Two-Photon Loss

Bernard Yurke and Eyal Buks

***Abstract*—Two-photon loss mechanisms often accompany a Kerr nonlinearity. The kinetic inductance exhibited by superconducting transmission lines provides an example of a Kerr-like nonlinearity that is accompanied by a nonlinear resistance of the two-photon absorptive type. Such nonlinear dissipation can degrade the performance of amplifiers and mixers employing a Kerr-like nonlinearity as the gain or mixing medium. As an aid for parametric-amplifier design, the authors provide a quantum analysis of a cavity parametric amplifier employing a Kerr nonlinearity that is accompanied by a two-photon absorptive loss. Because of their usefulness in diagnostics, we obtain expressions for the pump amplitude within the cavity, the reflection coefficient for the pump amplitude reflected off of the cavity, the parametric gain, and the intermodulation gain. Expressions by which the degree of squeezing can be computed are also presented. Although the focus here is on providing aids for the design of kinetic-inductance parametric amplifiers, much of what is presented is directly applicable to analogous optical and mechanical amplifiers.**

***Index Terms*—Kinetic inductance, noise squeezing, nonlinear, parametric amplifier.**

I. Introduction

SENSITIVE superconducting microwave devices, such as tunnel junction mixers [1], [2] and parametric amplifiers [3], [4], have been devised, which achieve performances close to the quantum limit. Phase-sensitive Josephson junction parametric amplifiers have been constructed whose noise performance exceeds that of the quantum limits imposed on linear phase-insensitive parametric amplifiers [5]. These phase-sensitive amplifiers have been used to generate quantum-mechanical states of the electromagnetic field, called squeezed states, whose noise in one amplitude component is reduced below that of vacuum fluctuations. The kinetic inductance of superconducting transmission lines could also be used to make low-noise parametric amplifiers. However, associated with the kinetic inductance is a nonlinear resistance that can degrade device performance. These nonlinear effects are relatively strong in superconducting striplines and microstrips due to the nonuniform distribution of the microwave current along the cross section of the transmission line. Along the edges, where the current density obtains its peak value, the current density can become overcritical, even with relatively moderate power levels. As a result, the superconducting-current density may vary, and consequently, both inductance L and resistance R per-unit length become current dependent according to the form [6]

$$L = L_0 + \Delta L \left(\frac{I}{I_c}\right)^2 \tag{1}$$

$$R = R_0 + \Delta R \left(\frac{I}{I_c}\right)^2 \tag{2}$$

where $I(I_c)$ is the total (critical) current. The kinetic inductance provides a Kerr-like nonlinearity suitable for the construction of parametric amplifiers, which employ four-wave mixing. The nonlinear resistance, to lowest order, is of the two-photon absorptive type. To aid in the design of parametric microwave amplifiers, which employ kinetic inductance, we have preformed an analysis of cavity parametric amplifiers employing a Kerr nonlinear element for gain and a two-photon absorptive loss. Although the analysis was carried out with a specific application in mind [7]–[10], it is more generally applicable, since two-photon absorptive processes often accompany Kerr nonlinearities. There are optical [11]–[13] and mechanical [14]–[17] systems with such combinations of nonlinearities.

Squeezing in a parametric amplifier with a two-photon absorber has been studied by a number of workers [13], [18]–[20]. In the analysis provided here, we present expressions for the amplitude of the pump field within the cavity, the reflection coefficient for the pump off the cavity, the intermodulation gain, and the degree of squeezing. The first, second, and third of these quantities are particularly useful for extracting model parameters from experimental data. The equations of motion are derived using the input–output theory of Gardiner and Collett [21], [22]. The undepleted pump approximation is then made, allowing the pump field inside the cavity and the pump field reflected from the cavity to be calculated. The small signal response is then obtained by linearization about the pump field.

II. Hamiltonian

A lossless transmission-line resonator having nonlinear kinetic inductance is discussed in Appendix A, and the effect of nonlinear losses associated with the kinetic inductance is

Manuscript received February 24, 2006; revised August 31, 2006. This work was supported in part by the German Israel Foundation under Grant 1-2038.1114.07, in part by the Israel Science Foundation under Grant 1380021, in part by the Deborah Foundation, and in part by the Poznanski Foundation.

B. Yurke is with the Bell Laboratories, Lucent Technologies, Murray Hill, NJ 07974 USA.

E. Buks is with the Department of Electrical Engineering, Technion–Israel Institute of Technology, Haifa 32000, Israel (e-mail: eyal@ee.technion.ac.il).

Color versions of all figures are available online at http://ieeexplore.ieee.org.
Digital Object Identifier 10.1109/JLT.2006.884490

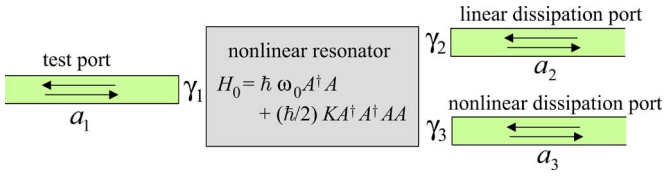

Fig. 1. Model includes a nonlinear resonator coupled to three ports. A test port; a linear-dissipation port; and a nonlinear-dissipation port.

discussed in Appendix B. Here, we consider the case where the external signals employed for driving the resonator are all close in frequency to one of the resonances at ω_0. As we discuss in the Appendices, under some conditions, which are assumed to be satisfied, all other modes of the resonator can be disregarded. In this case, the Hamiltonian of the nonlinear resonator can be written as [23], [24]

$$H_r = \hbar\omega_0 A^\dagger A + \frac{\hbar}{2} K A^\dagger A^\dagger A A \tag{3}$$

where the Kerr constant K is given in (150).

As shown in Fig. 1, the resonator is coupled to a test port (labeled as a_1) serving as the input–output port. Operated as an amplifier, the signal returned or "reflected" from the input port is larger than the incoming signal. This mode of operation, at microwave frequencies, is referred to as the negative-resistance reflection mode. Two extra fictitious ports are added in order to theoretically model dissipation [25]. Port a_2 serves as a linear loss port. Port a_3 serves as the two-photon loss port. The coupling of the a_3 loss mode to the resonator mode A is nonlinear and its Hamiltonian is given in (10).

It is convenient to write the Hamiltonian as a sum of terms

$$H = H_r + H_{a_1} + H_{a_2} + H_{a_3} + H_{T_1} + H_{T_2} + H_{T_3} \tag{4}$$

each representing the Hamiltonian for a component of the system.

The three ports coupled to the resonator (see Fig. 1) serve as baths. One bath models the external modes that couple to the resonator mode through the port that serves both as the input port and as the output port. The Hamiltonian H_{a1} for this bath is given by

$$H_{a1} = \int d\omega \hbar\omega a_1^\dagger(\omega) a_1(\omega). \tag{5}$$

The other two baths are associated with the linear and nonlinear cavity losses and their Hamiltonians are given by

$$H_{a2} = \int d\omega \hbar\omega a_2^\dagger(\omega) a_2(\omega) \tag{6}$$

and

$$H_{a3} = \int d\omega \hbar\omega a_3^\dagger(\omega) a_3(\omega). \tag{7}$$

The linear coupling of the bath modes a_1 and a_2 to the cavity mode A is modeled by the hopping Hamiltonians

$$H_{T_1} = \hbar \int d\omega \left[\kappa_1 A^\dagger a_1(\omega) + \kappa_1^* a_1^\dagger(\omega) A\right] \tag{8}$$

and

$$H_{T_2} = \hbar \int d\omega \left[\kappa_2 A^\dagger a_2(\omega) + \kappa_2^* a_2^\dagger(\omega) A\right]. \tag{9}$$

The two-photon absorptive coupling of the resonator mode to the bath modes a_3 is modeled by a hopping Hamiltonian in which two cavity photons are destroyed for every bath photon created [26]–[30]

$$H_{T_3} = \hbar \int d\omega \left[\kappa_3 A^\dagger A^\dagger a_3(\omega) + \kappa_3^* a_3^\dagger(\omega) A A\right]. \tag{10}$$

All the modes in this model satisfy the usual boson commutation relations.

III. The Equations of Motion

Since the creation and annihilation operators appearing in (3)–(10) do not have an explicit time dependence, the Heisenberg equation of motion for these operators has the form

$$i\hbar \frac{dO}{dt} = [O, H] \tag{11}$$

where H is the total Hamiltonian. Using the boson commutation relation for the cavity mode

$$[A, A^\dagger] = AA^\dagger - A^\dagger A = 1 \tag{12}$$

one has

$$\frac{dA}{dt} = -i\omega_0 A - iKA^\dagger AA - i\kappa_1 \int d\omega a_1(\omega) - i\kappa_2 \int d\omega a_2(\omega) - i2\kappa_3 \int d\omega A^\dagger a_3(\omega). \tag{13}$$

Using the boson-commutation relations for the bath modes

$$\left[a_i(\omega), a_j^\dagger(\omega')\right] = \delta_{i,j}\delta(\omega - \omega') \tag{14}$$

$$[a_i(\omega), a_j(\omega')] = 0 \tag{15}$$

one obtains the following equations for the bath modes $a_1(\omega)$, $a_2(\omega)$, and $a_3(\omega)$:

$$\frac{da_1(\omega)}{dt} = -i\omega a_1(\omega) - i\kappa_1^* A \tag{16}$$

$$\frac{da_2(\omega)}{dt} = -i\omega a_2(\omega) - i\kappa_2^* A \tag{17}$$

and

$$\frac{da_3(\omega)}{dt} = -i\omega a_3(\omega) - i\kappa_3^* AA. \tag{18}$$

Using the standard methods of Gardiner and Collett [21], these equations yield the following equation for the cavity mode A driven by the incoming bath modes a_i^{in}:

$$\frac{dA}{dt} = -i\omega_0 A - iKA^\dagger AA - \gamma A - \gamma_3 A^\dagger AA - i\sqrt{2\gamma_1}e^{i\phi_1}a_1^{\text{in}}(t) - i\sqrt{2\gamma_2}e^{i\phi_2}a_2^{\text{in}}(t) - i2\sqrt{\gamma_3}e^{i\phi_3}A^\dagger a_3^{\text{in}}(t) \tag{19}$$

where

$$\gamma = \gamma_1 + \gamma_2 \tag{20}$$

and the κ_i, which in general can be complex, have been reexpressed in terms of the positive real constants γ_i and the phases ϕ_i, according to

$$\kappa_1 = \sqrt{\frac{\gamma_1}{\pi}}e^{i\phi_1} \tag{21}$$

$$\kappa_2 = \sqrt{\frac{\gamma_2}{\pi}}e^{i\phi_2} \tag{22}$$

$$\kappa_3 = \sqrt{\frac{\gamma_3}{2\pi}}e^{i\phi_3}. \tag{23}$$

Expressions for γ_2 and γ_3 in terms of linear and nonlinear resistance of the stripline [see (2)] are given in (165) and (166) of Appendix B. In addition, the methods of Gardiner and Collett [21] yield the following relations between the outgoing bath modes a_i^{out}, the incoming bath modes a_i^{in}, and the cavity mode A:

$$a_1^{\text{out}}(t) - a_1^{\text{in}}(t) = -i\sqrt{2\gamma_1}e^{-i\phi_1}A(t) \tag{24}$$

$$a_2^{\text{out}}(t) - a_2^{\text{in}}(t) = -i\sqrt{2\gamma_2}e^{-i\phi_2}A(t) \tag{25}$$

$$a_3^{\text{out}}(t) - a_3^{\text{in}}(t) = -i\sqrt{\gamma_3}e^{-i\phi_3}A(t)A(t). \tag{26}$$

In obtaining these equations, a Markov approximation [21] has been made such that the boson-annihilation operators $a_i^{\text{in}}(t)$ satisfy the commutation relations

$$\left[a_i^{\text{in}}(t), a_j^{\text{in}\dagger}(t')\right] = \delta_{i,j}\delta(t-t') \tag{27}$$

$$\left[a_i^{\text{in}}(t), a_j^{\text{in}}(t')\right] = 0. \tag{28}$$

IV. Response to a Classical Pump

Operated as a negative-resistance reflection amplifier, an intense sinusoidal field, called the pump, is delivered to the input port of the device. Signals having frequencies to either side of the pump, but lying within the bandwidth of the device, will be amplified. The linearization procedure is now carried out in which the signals entering the input port and the noise entering the loss ports are considered to be small compared to the pump. The first step is to calculate the classical response of the device to an intense pump in the absence of signal and noise. The solution is then used to calculate the linearized response of the device in the presence of signal and noise.

In order to obtain the response of the device to a classical pump in the absence of signal and noise, one sets the incoming noise terms to zero

$$a_2^{\text{in}} = 0 \tag{29}$$

$$a_3^{\text{in}} = 0. \tag{30}$$

The incoming pump is written as

$$a_1^{\text{in}} = b_1^{\text{in}}e^{-i(\omega_p t + \psi_1)} \tag{31}$$

where b_1^{in} is a real constant, ω_p is the pump frequency, and ψ_1 is the pump phase. The outgoing field will also have an oscillatory time dependence of frequency ω_p and can be written as

$$a_1^{\text{out}} = b_1^{\text{out}}e^{-i(\omega_p t + \psi_1)} \tag{32}$$

where b_1^{out} may be a complex constant. Writing A as

$$A = Be^{-i(\omega_p t + \phi_B)} \tag{33}$$

where B is a positive real constant, the equations of motion (19) and (24) yield

$$[i(\omega_0 - \omega_p) + \gamma]B + (iK + \gamma_3)B^3 = -i\sqrt{2\gamma_1}b_1^{\text{in}}e^{i(\phi_1 + \phi_B - \psi_1)} \tag{34}$$

and

$$b_1^{\text{out}} = b_1^{\text{in}} - i\sqrt{2\gamma_1}Be^{-i(\phi_1 + \phi_B - \psi_1)}. \tag{35}$$

Multiplying each side of (34) by its complex conjugate and introducing

$$E = B^2 \tag{36}$$

one obtains

$$E^3 + \frac{2\left[(\omega_0 - \omega_p)K + \gamma\gamma_3\right]}{K^2 + \gamma_3^2}E^2 + \frac{(\omega_0 - \omega_p)^2 + \gamma^2}{K^2 + \gamma_3^2}E - \frac{2\gamma_1}{K^2 + \gamma_3^2}\left(b_1^{\text{in}}\right)^2 = 0. \tag{37}$$

This cubic equation will have either one real solution and two complex solutions or three real solutions. For the case when two of the solutions are complex, the real solution is the physical solution. If there are three real solutions, two will be stable, and one will be unstable, and the device will exhibit bistability. Once E and, hence, B have been determined from (37) and (36), the phase ϕ_B can be determined from (34), and the amplitude of the reflected pump can then be computed from (35). In Fig. 2(a), (d), and (g), plots of B as a function of frequency for three different incoming pump amplitudes are shown. The frequency pulling of the cavity resonance is clearly shown in Fig. 2(d) and (g) as the incoming pump amplitude b_1^{in} is increased. Also, plotted in Fig. 2(b), (e), and (h) is the reflection coefficient $|b_1^{\text{out}}/b_1^{\text{in}}|$ for the reflected pump amplitude as a function of frequency. If no power were absorbed by the cavity, the reflection coefficient would be unity. One sees a dip in the reflected power at the cavity resonance. As the incoming

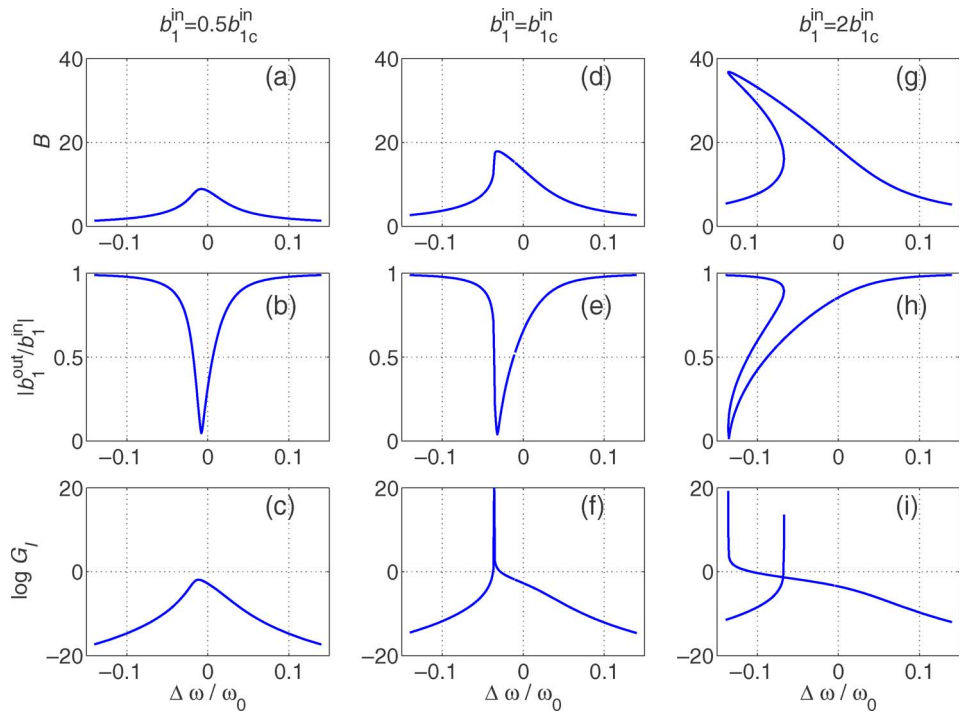

Fig. 2. Cavity-mode amplitude B, the reflection amplitude $|b_1^{\rm out}/b_1^{\rm in}|$, and the intermodulation gain G_I for vanishing offset frequency $\omega = 0$ shown for subcritical case $b_1^{\rm in} = 0.5b_{1c}^{\rm in}$, critical case $b_1^{\rm in} = b_{1c}^{\rm in}$, and above-critical case $b_1^{\rm in} = 2b_{1c}^{\rm in}$. In all cases, $K = -10^{-4}\omega_0$, $\gamma_1 = 0.01\omega_0$, $\gamma_2 = 1.1\gamma_1$, and $\gamma_3 = 0.01K/\sqrt{3}$. For $b_1^{\rm in} > b_{1c}^{\rm in}$, the response becomes a multivalue function of frequency in a particular frequency range.

pump amplitude is increased, this absorption feature also shows frequency pulling, as shown in Fig. 2(e) and (h).

A. Special Operating Points

As a function of the pump frequency ω_p, B will have the form of the distorted Lorentzian curve [see Fig. 2(a), (d), and (g)] exhibited by Duffing oscillators [31]–[33]. The maximum of the response curve occurs when $\partial E/\partial\omega_p = 0$. This condition yields

$$\omega_0 - \omega_p + KE = 0 \tag{38}$$

that is, the peak of the resonance curve is shifted by an amount KB^2. The points of instability, where the system will switch from one of the two bistable states to the other, are located where $\partial\omega_p/\partial E = 0$. This condition is satisfied when

$$(\gamma + 2\gamma_3 E)^2 = \left(K^2 + \gamma_3^2\right)E^2 - (\omega_0 - \omega_p + 2KE)^2. \tag{39}$$

When, in addition, $\partial^2\omega_p/\partial E^2 = 0$, the two points of instability coalesce into a single point. The condition $\partial^2\omega_p/\partial E^2 = 0$ is satisfied when

$$6\left(K^2 + \gamma_3^2\right)E + 4\left[(\omega_0 - \omega_p)K + \gamma\gamma_3\right] = 0. \tag{40}$$

Large parametric gain is achieved at points where the slope of E with respect to ω_p becomes infinite, but in order to remain stable, it is desirable to operate the reflection parametric amplifier near the critical point with parameters chosen so that the Duffing curve does not have a bistable region. It is a straightforward exercise to show that in order for the resonance curve to have a critical point at which both (39) and (40) are satisfied, one must have

$$|K| > \sqrt{3}\gamma_3. \tag{41}$$

At the critical point one has

$$E_c = \frac{2\gamma}{\sqrt{3}\left(|K| - \sqrt{3}\gamma_3\right)} \tag{42}$$

and

$$\omega_0 - \omega_p = -\gamma\frac{K}{|K|}\left[\frac{4\gamma_3|K| + \sqrt{3}\left(K^2 + \gamma_3^2\right)}{K^2 - 3\gamma_3^2}\right]. \tag{43}$$

The incoming pump amplitude required for operation at the critical point is given by

$$\left(b_{1c}^{\rm in}\right)^2 = \frac{4}{3\sqrt{3}}\frac{\gamma^3\left(K^2 + \gamma_3^2\right)}{\gamma_1\left(|K| - \sqrt{3}\gamma_3\right)^3}. \tag{44}$$

Thus, the input power required for driving the system into the threshold of bistability (critical point) is increased in the presence of two-photon losses. Moreover, when γ_3 exceeds the

value of $|K|/\sqrt{3}$, the bistability regime becomes inaccessible [see (41)]. When $\gamma_3 = 0$, these reduce to

$$E_c = \frac{2\sqrt{3}\gamma}{3|K|} \tag{45}$$

$$\omega_0 - \omega_p = -\sqrt{3}\gamma\frac{K}{|K|} \tag{46}$$

$$\left(b_{1c}^{\text{in}}\right)^2 = \frac{4}{3\sqrt{3}}\frac{\gamma^3}{\gamma_1|K|}. \tag{47}$$

In Fig. 2(d), the amplitude of the cavity mode as a function of frequency has been plotted for the case when the incoming pump amplitude is that of the critical pump amplitude. One sees that the line shape of the cavity mode is vertical at a point on the lower side of the resonance. The line shape of the reflected power is shown in Fig. 2(e).

V. Linearization

A linearized analysis is now performed in which the incoming signal and the noise from the losses are regarded as small compared to the pump. To that end, we write

$$a_1^{\text{in}} = b_1^{\text{in}}e^{-i(\omega_p t+\psi_1)} + c_1^{\text{in}}e^{-i\omega_p t} \tag{48}$$

$$a_2^{\text{in}} = c_2^{\text{in}}e^{-i\omega_p t} \tag{49}$$

$$a_3^{\text{in}} = c_3^{\text{in}}e^{-i\omega_p t} \tag{50}$$

$$a_1^{\text{out}} = b_1^{\text{out}}e^{-i(\omega_p t+\psi_1)} + c_1^{\text{out}}e^{-i\omega_p t} \tag{51}$$

$$a_2^{\text{out}} = b_2^{\text{out}}e^{-i\omega_p t} + c_2^{\text{out}}e^{-i\omega_p t} \tag{52}$$

$$a_3^{\text{out}} = b_3^{\text{out}}e^{-i\omega_p t} + c_3^{\text{out}}e^{-i\omega_p t} \tag{53}$$

and

$$A = Be^{-i(\omega_p t+\phi_B)} + ae^{-i\omega_p t} \tag{54}$$

where B, b_1^{out}, b_2^{out}, and b_3^{out} constitute the solution for the response of the system to a classical pump in the absence of signal and noise. The properties of this solution have already been discussed in Section IV. The c_1^{in}, c_2^{in}, c_3^{in},c_1^{out}, c_2^{out}, c_3^{out}, and a are regarded as small and will be kept only up to linear order. Substituting these into the equations of motion yields

$$\begin{aligned}\frac{da}{dt} =& -\left[i(\omega_0-\omega_p)+\gamma\right]a - 2(iK+\gamma_3)B^2a \\ & -(iK+\gamma_3)B^2e^{-i2\phi_B}a^\dagger - i\sqrt{2\gamma_1}e^{i\phi_1}c_1^{\text{in}} \\ & -i\sqrt{2\gamma_2}e^{i\phi_2}c_2^{\text{in}} - i2\sqrt{\gamma_3}Be^{i(\omega_p t+\phi_B+\phi_3)}c_3^{\text{in}}\end{aligned} \tag{55}$$

$$c_1^{\text{out}} - c_1^{\text{in}} = -i\sqrt{2\gamma_1}e^{-i\phi_1}a \tag{56}$$

$$c_2^{\text{out}} - c_2^{\text{in}} = -i\sqrt{2\gamma_2}e^{-i\phi_2}a \tag{57}$$

$$c_3^{\text{out}} - c_3^{\text{in}} = -i2\sqrt{\gamma_3}Be^{-i(\omega_p t+\phi_B+\phi_3)}a. \tag{58}$$

VI. Solving the Linearized Equation

Introducing

$$W = i(\omega_0-\omega_p) + \gamma + 2(iK+\gamma_3)B^2 \tag{59}$$

$$V = (iK+\gamma_3)B^2e^{-2i\phi_B} \tag{60}$$

and

$$F = -i\sqrt{2\gamma_1}e^{i\phi_1}c_1^{\text{in}} - i\sqrt{2\gamma_2}e^{i\phi_2}c_2^{\text{in}} - i2\sqrt{\gamma_3}Be^{i(\omega_p t+\phi_B+\phi_3)}c_3^{\text{in}} \tag{61}$$

the linearized equation of motion can be written in the form

$$\frac{da}{dt} + Wa + Va^\dagger = F. \tag{62}$$

From this last equation, one obtains

$$\frac{d^2a}{dt^2} + 2\Re(W)\frac{da}{dt} + \left(|W|^2 - |V|^2\right)a = \Gamma(t) \tag{63}$$

where

$$\Gamma(t) = \frac{dF}{dt} + W^*F - VF^\dagger(t). \tag{64}$$

Writing

$$a = e^{-\lambda t} \tag{65}$$

the characteristic equation for the homogenous equation is given by

$$\lambda^2 - 2\Re(\omega)\lambda + |W|^2 - |V|^2 = 0. \tag{66}$$

This has the two roots

$$\lambda_0 = \Re(W) - \sqrt{\Re^2(W) - |W|^2 + |V|^2)} \tag{67}$$

$$\lambda_1 = \Re(W) + \sqrt{\Re^2(W) - |W|^2 + |V|^2)} \tag{68}$$

or

$$\lambda_0 = \gamma + 2\gamma_3B^2 - \sqrt{\left(K^2+\gamma_3^2\right)B^4 - (\omega_0-\omega_p+2KB^2)^2} \tag{69}$$

$$\lambda_1 = \gamma + 2\gamma_3B^2 + \sqrt{\left(K^2+\gamma_3^2\right)B^4 - (\omega_0-\omega_p+2KB^2)^2}. \tag{70}$$

The root λ_0 is zero when (39) is satisfied, that is, one has critical slowing down at the points, where the slope of E with respect to ω_p is infinite.

Introducing the Fourier transforms

$$a(t) = \frac{1}{\sqrt{2\pi}}\int_{-\infty}^{\infty} d\omega a(\omega)e^{-i\omega t} \tag{71}$$

$$c_1(t) = \frac{1}{\sqrt{2\pi}}\int_{-\infty}^{\infty} d\omega c_1(\omega)e^{-i\omega t} \tag{72}$$

$$c_2(t) = \frac{1}{\sqrt{2\pi}} \int_{-\infty}^{\infty} d\omega c_2(\omega) e^{-i\omega t} \tag{73}$$

$$c_3(t) = \frac{1}{\sqrt{2\pi}} \int_{-\infty}^{\infty} d\omega c_3(\omega) e^{-i\omega t} \tag{74}$$

$$\Gamma(t) = \frac{1}{\sqrt{2\pi}} \int_{-\infty}^{\infty} d\omega \Gamma(\omega) e^{-i\omega t} \tag{75}$$

(63) yields

$$a(\omega) = \frac{\Gamma(\omega)}{-\omega^2 - 2i\omega\Re(W) + (|W|^2 - |V|^2)}. \tag{76}$$

In terms of the roots of the characteristic equation, this can be written as

$$a(\omega) = \frac{\Gamma(\omega)}{(-i\omega + \lambda_0)(-i\omega + \lambda_1)} \tag{77}$$

where

$$\begin{aligned}\Gamma(\omega) = &- i\sqrt{2\gamma_1}\left[(-i\omega + W^*)e^{i\phi_1} c_1^{\text{in}}(\omega) - Ve^{-i\phi_1} c_1^{\text{in}\dagger}(-\omega)\right] \\ &- i\sqrt{2\gamma_2}\left[(-i\omega + W^*)e^{i\phi_2} c_2^{\text{in}}(\omega) - Ve^{-i\phi_2} c_2^{\text{in}\dagger}(-\omega)\right] \\ &- i2\sqrt{\gamma_3}B\left[(-i\omega + W^*)e^{i(\phi_B+\phi_3)} c_3^{\text{in}}(\omega_p + \omega)\right. \\ &\left. - Ve^{-i(\phi_B+\phi_3)} c_3^{\text{in}\dagger}(\omega_p - \omega)\right].\end{aligned} \tag{78}$$

A. Output Field

From (24), one obtains

$$c_1^{\text{out}}(\omega) = c_1^{\text{in}}(\omega) - i\sqrt{2\gamma_1} e^{-i\phi_1} a(\omega). \tag{79}$$

Substituting (77) into this equation yields

$$c_1^{\text{out}}(\omega) = \frac{(-i\omega + \lambda_0)(-i\omega + \lambda_1) c_1^{\text{in}}(\omega) - i\sqrt{2\gamma_1} e^{-i\phi_1} \Gamma(\omega)}{(-i\omega + \lambda_0)(-i\omega + \lambda_1)} \tag{80}$$

or

$$\begin{aligned}&c_1^{\text{out}}(\omega) \\ &\quad = \frac{(-i\omega + \lambda_0)(-i\omega + \lambda_1) - 2\gamma_1(-i\omega + W^*)}{(-i\omega + \lambda_0)(-i\omega + \lambda_1)} c_1^{\text{in}}(\omega) \\ &\qquad + \frac{2\gamma_1 V e^{-i2\phi_1}}{(-i\omega + \lambda_0)(-i\omega + \lambda_1)} c_1^{\text{in}\dagger}(-\omega) \\ &\qquad - \frac{2\sqrt{\gamma_1\gamma_2}(-i\omega + W^*)e^{-i(\phi_1 - \phi_2)}}{(-i\omega + \lambda_0)(-i\omega + \lambda_1)} c_2^{\text{in}}(\omega) \\ &\qquad + \frac{2\sqrt{\gamma_1\gamma_2} V e^{-i(\phi_1 + \phi_2)}}{(-i\omega + \lambda_0)(-i\omega + \lambda_1)} c_2^{\text{in}\dagger}(-\omega) \\ &\qquad - \frac{2\sqrt{2\gamma_1\gamma_3}B(-i\omega + W^*)e^{-i(\phi_1 - \phi_B - \phi_3)}}{(-i\omega + \lambda_0)(-i\omega + \lambda_1)} c_3^{\text{in}}(\omega_p + \omega) \\ &\qquad + \frac{2\sqrt{2\gamma_1\gamma_3}BVe^{-i(\phi_1 + \phi_3 + \phi_B)}}{(-i\omega + \lambda_0)(-i\omega + \lambda_1)} c_3^{\text{in}\dagger}(\omega_p - \omega).\end{aligned} \tag{81}$$

The linearized solution to the equations of motion has now been obtained. We will now evaluate the properties of this solution for various kinds of inputs.

VII. Parametric and Intermodulation Gain

The parametric gain and the intermodulation gain are calculated by taking $c_1^{\text{in}}(\omega)$ to represent a classical signal at frequency $\omega_p + \omega$. Setting all other signal and noise inputs to zero, (81) yields the following power gain for the reflected signal:

$$\begin{aligned}G_S &\equiv \frac{\left|c_1^{\text{out}}(\omega)\right|^2}{\left|c_1^{\text{in}}(\omega)\right|^2} \\ &= \frac{\left|(-i\omega + \lambda_0)(-i\omega + \lambda_1) - 2\gamma_1(-i\omega + W^*)\right|^2}{(\omega^2 + \lambda_0^2)(\omega^2 + \lambda_1^2)}.\end{aligned} \tag{82}$$

When this quantity becomes greater than unity, one has parametric amplification of the signal.

As shown from (81), a signal $c_{\text{in}}(-\omega)$ injected at frequency $\omega_p - \omega$ will generate an output signal at frequency $\omega_p + \omega$. This frequency conversion is quantified by the intermodulation-conversion gain defined by

$$\begin{aligned}G_I &\equiv \frac{\left|c_1^{\text{out}}(\omega)\right|^2}{\left|c_1^{\text{in}}(-\omega)\right|^2} \\ &= \frac{4\gamma_1^2|V|^2}{(\omega^2 + \lambda_0^2)(\omega^2 + \lambda_1^2)}.\end{aligned} \tag{83}$$

Since the output signal at $\omega_p + \omega$ is separated in frequency from the input signal, the measurement of the intermodulation gain is a particularly sensitive method for measuring the strength of the nonlinearities. We note that, even without power gain, devices capable of producing intermodulation signals are useful as mixers. When $\omega = 0$, both the expression for G_S and the expression for G_I will have $\lambda_0^2\lambda_1^2$ in the denominator. As one approaches an operating point where the slope of E with respect to ω_p becomes infinite, both the parametric gain and the intermodulation-conversion gain will diverge. Hence, it is near the instability points where the device can exhibit large gains. Fig. 2(c), (f), and (i) shows the behavior of the intermodulation gain as the pump amplitude is increased from half critical [Fig. 2(c)] to critical [Fig. 2(f)] to twice critical [Fig. 2(i)] as a function of frequency. As depicted in [Fig. 2(f)] at the critical point the intermodulation gain diverges. Above critical, as shown in [Fig. 2(i)], the intermodulation gain diverges as one approaches the points of infinite slope on the resonance curve [Fig. 2(g)].

VIII. Noise Squeezing

Because of intermodulation gain, a parametric amplifier can establish correlations [34] between the output at $\omega_p + \omega$ and $\omega_p - \omega$. When delivered to a mixer whose local oscillator is phase locked to the pump, these correlations can result in noise fluctuations reduced below that which the mixer would see if the signal delivered to the parametric amplifier were, instead,

directly delivered to the mixer. This noise reduction is called squeezing, and it can occur with either thermal or quantum noise [5]. We now obtain expressions that will allow one to calculate the degree of thermal or quantum noise squeezing. For such a calculation, the $c_1^{\rm in}$, $c_2^{\rm in}$, $c_3^{\rm in}$, $c_1^{\rm out}$, $c_2^{\rm out}$, and $c_3^{\rm out}$ are again treated as quantum-mechanical operators satisfying commutation relations of the form (27) and (28).

The output of a mixer, operated in the homodyne mode in which the local oscillator frequency $\omega_{\rm LO}$ and the pump frequency ω_p are equal and in which the input at the signal frequency $\omega_{\rm LO}+\omega$ and at the image frequency $\omega_{\rm LO}-\omega$ are both regarded as signal, is given by [4]

$$I_D(\omega)=c_1^{\rm out\dagger}(-\omega)e^{-i\phi_{\rm LO}}+c_1^{\rm out}(\omega)e^{i\phi_{\rm LO}} \tag{84}$$

where $\phi_{\rm LO}$ is the local oscillator phase. To evaluate the mean value and the power spectrum for the homodyne-detector output, it is necessary to specify the density matrix for the signal and noise entering the parametric amplifier. Here, we consider the case when these inputs consist of Nyquist noise. In this case, one has

$$\left\langle c_i^{\rm in}(\omega)\right\rangle=0 \tag{85}$$

$$\left\langle c_i^{\rm in\dagger}(\omega)c_j^{\rm in}(\omega')\right\rangle=\frac{e^{-\beta_i\hbar\omega_p}}{1-e^{-\beta_i\hbar\omega_p}}\delta_{i,j}\delta(\omega-\omega') \tag{86}$$

and

$$\left\langle c_i^{\rm in}(\omega)c_j^{\rm in}(\omega')\right\rangle=0. \tag{87}$$

Here

$$\beta_i=\frac{1}{k_BT_i} \tag{88}$$

where k_B is the Boltzmann's constant, and T_i is the absolute temperature of the bath for which $c_i^{\rm in}(\omega)$ is the incoming mode. We, thus, allow each of the baths to be at a different temperature. In writing (86), we have made the approximation that the frequencies ω of interest are small compared to ω_p.

Because (81) is linear in the $c_i^{\rm in}(\omega)$, it is evident that

$$\langle I_D(\omega)\rangle=0 \tag{89}$$

that is, the homodyne-detector output consists of noise fluctuations with zero mean. Because of the boson-commutation relations, one has

$$\left\langle I_D^\dagger(\omega)I_D(\omega')\right\rangle=P(\omega)\delta(\omega-\omega') \tag{90}$$

where $P(\omega)$ is the noise-power spectrum of the homodyne-detector output. Equation (81) can be rewritten as

$$\begin{aligned}c_1^{\rm out}(\omega)&=A_1(\omega)c_1^{\rm in}(\omega)+B_1(\omega)c_1^{\rm in\dagger}(-\omega)+A_2(\omega)c_2^{\rm in}(\omega)\\&+B_2(\omega)c_2^{\rm in\dagger}(-\omega)+A_3(\omega)c_3^{\rm in}(\omega_p+\omega)+B_3(\omega)c_3^{\rm in\dagger}(\omega_p-\omega)\end{aligned} \tag{91}$$

where

$$A_1(\omega)=\frac{(-i\omega+\lambda_0)(-i\omega+\lambda_1)-2\gamma_1(-i\omega+W^*)}{(-i\omega+\lambda_0)(-i\omega+\lambda_1)} \tag{92}$$

$$B_1(\omega)=\frac{2\gamma_1Ve^{-i2\phi_1}}{(-i\omega+\lambda_0)(-i\omega+\lambda_1)} \tag{93}$$

$$A_2(\omega)=-\frac{2\sqrt{\gamma_1\gamma_2}(-i\omega+W^*)e^{-i(\phi_1-\phi_2)}}{(-i\omega+\lambda_0)(-i\omega+\lambda_1)} \tag{94}$$

$$B_2(\omega)=\frac{2\sqrt{\gamma_1\gamma_2}Ve^{-i(\phi_1+\phi_2)}}{(-i\omega+\lambda_0)(-i\omega+\lambda_1)} \tag{95}$$

$$A_3(\omega)=-\frac{2\sqrt{2\gamma_1\gamma_3}B(-i\omega+W^*)e^{-i(\phi_1-\phi_B-\phi_3)}}{(-i\omega+\lambda_0)(-i\omega+\lambda_1)} \tag{96}$$

$$B_3(\omega)=\frac{2\sqrt{2\gamma_1\gamma_3}BVe^{-i(\phi_1+\phi_3+\phi_B)}}{(-i\omega+\lambda_0)(-i\omega+\lambda_1)}. \tag{97}$$

Substituting (91) into (84), evaluating $\langle I_D^\dagger(\omega)I_D(\omega')\rangle$ using (86), and then reading off the power spectrum using (90), one obtains

$$\begin{aligned}P(\omega)=&\left|e^{-i\phi_{\rm LO}}A_1^*(\omega)+e^{i\phi_{\rm LO}}B_1(-\omega)\right|^2\frac{e^{-\beta_1\hbar\omega_p}}{1-e^{-\beta_1\hbar\omega_p}}\\&+\left|e^{i\phi_{\rm LO}}A_1(-\omega)+e^{-i\phi_{\rm LO}}B_1^*(\omega)\right|^2\frac{1}{1-e^{-\beta_1\hbar\omega_p}}\\&+\left|e^{-i\phi_{\rm LO}}A_2^*(\omega)+e^{i\phi_{\rm LO}}B_2(-\omega)\right|^2\frac{e^{-\beta_2\hbar\omega_p}}{1-e^{-\beta_2\hbar\omega_p}}\\&+\left|e^{i\phi_{\rm LO}}A_2(-\omega)+e^{-i\phi_{\rm LO}}B_2^*(\omega)\right|^2\frac{1}{1-e^{-\beta_2\hbar\omega_p}}\\&+\left|e^{-i\phi_{\rm LO}}A_3^*(\omega)+e^{i\phi_{\rm LO}}B_3(-\omega)\right|^2\frac{e^{-\beta_3\hbar\omega_p}}{1-e^{-\beta_3\hbar\omega_p}}\\&+\left|e^{i\phi_{\rm LO}}A_3(-\omega)+e^{-i\phi_{\rm LO}}B_3^*(\omega)\right|^2\frac{1}{1-e^{-\beta_3\hbar\omega_p}}.\end{aligned} \tag{98}$$

This formula may be used to compute the noise-power spectrum for any local oscillator phase $\phi_{\rm LO}$ and any set of device parameters. It is useful to consider the case when there is no incoming pump field and the input field and loss baths are all at zero temperature. In this case, the field reflected off the input port of the amplifier will consist of vacuum fluctuations, that is

$$c_1^{\rm out}(\omega)|0\rangle=0 \tag{99}$$

and one obtains

$$\left\langle I_D^\dagger(\omega)I_D(\omega')\right\rangle=\delta(\omega-\omega') \tag{100}$$

or

$$P(\omega)=1. \tag{101}$$

This sets the vacuum-noise level for the conventions we are using. As shown in Fig. 3 and as will be illustrated with specific examples in the next section, under suitable circumstances, it is possible to obtain reflected signals whose noise-power spectrum $P(\omega)$, for certain local oscillator-phase settings, is

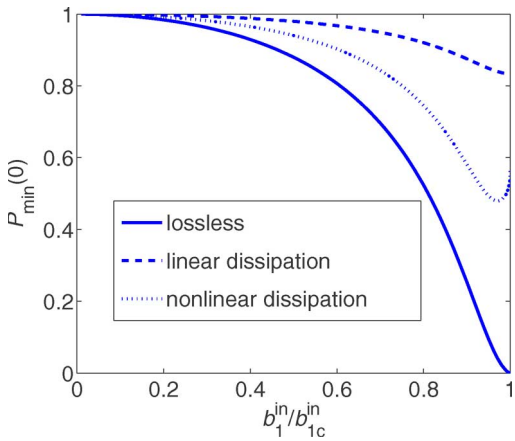

Fig. 3. Examples of achievable degree of squeezing $P_{\min}(0)$ versus $b_1^{\rm in}/b_{1c}^{\rm in}$. In all plots, $T_1 = T_2 = T_3 = 0$, $K = 5\omega_0$, $\gamma_1 = 0.0001\omega_0$, and the pump frequency ω_p obtains its critical value, as given by (43). The solid line represents the lossless case, where $\gamma_2 = \gamma_3 = 0$. The dashed line represents the case of linear dissipation, where $\gamma_2 = 5\gamma_1$ and $\gamma_3 = 0$, while the dotted line represents the case of nonlinear dissipation, where $\gamma_2 = 0$ and $\gamma_3 = 0.5K/\sqrt{3}$.

less than one. Such signals are said to be squeezed below the vacuum-noise level. Fig. 3 shows the minimum value of $P(\omega)$ as a function of the amplitude of the incoming pump $b_1^{\rm in}$ when the bath temperatures are all zero, the strength of the Kerr nonlinearity is chosen to be $K = 5\omega_0$, and the coupling strength of the signal to the cavity mode is taken to be $\gamma_1 = 0.0001\omega_0$. The pump frequency has been chosen to be that of the critical pump frequency. The solid line is the lossless case when $\gamma_2 = \gamma_3 = 0$. In this case, complete squeezing $P(0) = 0$ is possible when the incoming pump power is at the critical value, that is, $|b_1^{\rm in}/b_{1c}^{\rm in}| = 1$. The dashed curve represents the case when the linear dissipation is given by $\gamma_2 = 5\gamma_1$ and the nonlinear dissipation γ_3 is zero. In general, the presence of linear dissipation reduces the amount of achievable squeezing. The dotted line depicts the case when the linear dissipation is zero and the nonlinear dissipation is given by $\gamma_3 = 0.5K/\sqrt{3}$. Nonlinear dissipation also tends to reduce the amount of squeezing that can be produced. However, nonlinear dissipation can produce some squeezing in the absence of a Kerr medium, as we discuss below.

A. Special Cases

It is instructive to evaluate (98) for a few specific cases. In particular, the power spectrum at $\omega = 0$ reduces to

$$P(0) = \left|e^{-i\phi_{\rm LO}}A_1^*(0) + e^{i\phi_{\rm LO}}B_1(0)\right|^2 \coth\left(\frac{\hbar\omega_p}{2k_BT_1}\right) + \left|e^{-i\phi_{\rm LO}}A_2^*(0) + e^{i\phi_{\rm LO}}B_2(0)\right|^2 \coth\left(\frac{\hbar\omega_p}{2k_BT_2}\right) + \left|e^{-i\phi_{\rm LO}}A_3^*(0) + e^{i\phi_{\rm LO}}B_3(0)\right|^2 \coth\left(\frac{\hbar\omega_p}{2k_BT_3}\right). \tag{102}$$

Further simplification results from considering the case when the internal losses are all zero. In this case, $\gamma_2 = 0$, and $\gamma_3 = 0$. Thus, the terms in (102) corresponding to internally generated noise vanish, and one obtains

$$P(0) = |e^{-i\phi_{\rm LO}}A_1^*(0) + e^{i\phi_{\rm LO}}B_1(0)|^2 \coth\left(\frac{\hbar\omega_p}{2k_BT_1}\right). \tag{103}$$

Writing

$$A_1(0) = |A_1(0)|\, e^{i\phi_A} \tag{104}$$

$$B_1(0) = |B_1(0)|\, e^{i\phi_B} \tag{105}$$

one has

$$P(0) = \left||A_1(0)| + |B_1(0)|\, e^{i\psi}\right|^2 \coth\left(\frac{\hbar\omega_p}{2k_BT_1}\right) \tag{106}$$

where

$$\psi = 2\phi_{\rm LO} - \phi_A + \phi_B. \tag{107}$$

$P(0)$ is maximized when the local oscillator phase $\phi_{\rm LO}$ is chosen so that

$$e^{i\psi} = 1. \tag{108}$$

In this case, one obtains

$$P_{\max}(0) = (|A_1(0)| + |B_1(0)|)^2 \coth\left(\frac{\hbar\omega_p}{2k_BT_1}\right). \tag{109}$$

$P(0)$ is minimized when the local oscillator phase $\phi_{\rm LO}$ is chosen so that

$$e^{i\psi} = -1. \tag{110}$$

In this case, one obtains

$$P_{\min}(0) = (|A_1(0)| - |B_1(0)|)^2 \coth\left(\frac{\hbar\omega_p}{2k_BT_1}\right). \tag{111}$$

From (107), (108), and (110), it follows that the local oscillator phase, at which the spectral density $P(0)$ is minimized, differs by $\pi/2$ from the local oscillator phase at which the spectral density is maximized, that is, the signal components minimizing and maximizing the spectral density are in quadrature. It is straightforward to show that

$$|A_1(0)|^2 - |B_1(0)|^2 = 1. \tag{112}$$

From this equation and (109) and (111), one obtains

$$P_{\max}(0)P_{\min}(0) = \coth^2\left(\frac{\hbar\omega_p}{2k_BT_1}\right). \tag{113}$$

Hence, in the case of no loss, the degree of amplification and the degree of deamplification of the noise are the same. For this case, one also has

$$|B_1(0)| = \frac{2\gamma_1 KB^2}{(\omega_0 - \omega_p + 2KB^2)^2 + \gamma_1^2 - K^2B^4}. \tag{114}$$

Note that $|B_1(0)|$ can be made arbitrarily large by choosing the pump frequency ω_p and the pump amplitude B such that the denominator goes to zero. From this, it follows that $P_{\max}$ can be made arbitrarily large, and $P_{\min}$ can be made arbitrarily small. In practice, higher order terms responsible for pump depletion will limit how big $P_{\max}$ can be made.

Noise from the losses and gain saturation will limit the maximum degree of noise squeezing to be below that calculated here. This is demonstrated in Fig. 3, where the achievable degree of squeezing $P_{\min}(0)$ is plotted as a function of $b_1^{\text{in}}/b_{1c}^{\text{in}}$ for some examples in which the linear or nonlinear loss is taken to be nonzero.

The presence of a two-photon loss allows for squeezing even in the absence of a Kerr nonlinearity [29]. Setting $K = 0$, $\gamma_2 = 0$, and $\omega_0 = \omega_p$, the greatest degree of squeezing of the output field of the cavity occurs when $\gamma_1 = 3\gamma_3 B^2$. At this operating point, $P(0) = 2/3$, and the local oscillator phase must be adjusted so that $\cos(2\phi_{\text{LO}} - 2\phi_B - 2\phi_1) = 1$.

IX. Conclusion

We have presented an analysis of a cavity parametric amplifier employing a Kerr nonlinearity, but which also possesses a two-photon loss. We have obtained expressions for the pump amplitude inside the cavity and the reflected pump amplitude for the case when pump saturation can be neglected. We have obtained expressions for the classical gain and the intermodulation gain. These expressions are useful for determining model parameters from experimental data. We have found that in the presence of two-photon losses, the injected power required for driving the system into the bistable regime is increased. Moreover, this regime becomes inaccessible when γ_3 exceeds the value of $|K|/\sqrt{3}$.

We have also obtained expressions from which one can compute the degree of squeezing that the device exhibits. Both the linear loss and the nonlinear loss tend to degrade the amount of squeezing that can be achieved, although even without a Kerr nonlinearity, a modest amount of squeezing can be achieved by the two-photon loss.

Appendix A
Nonlinear Kinetic Inductance in Transmission-Line Resonator

Consider a lossless linear transmission line with length l extending along the x-axis. Let $q(x,t)$ be the charge-density per-unit length, and define [25]

$$Q(x,t) = \int_x^\infty dx' q(x',t). \tag{115}$$

Thus, $q = -\partial Q/\partial x$, and the voltage across the transmission line is given by

$$V(x,t) = -\frac{1}{C}\frac{\partial Q}{\partial x} \tag{116}$$

where C is the capacitance-per-unit length along the transmission line, whereas the current is given by

$$I(x,t) = \frac{\partial Q}{\partial t}. \tag{117}$$

The Lagrangian $\mathcal{L}$ of the system reads

$$\begin{aligned}\mathcal{L} &= \frac{1}{2}\int_0^l dx[LI^2 - CV^2] \\ &= \frac{1}{2}\int_0^l dx\left[L\left(\frac{\partial Q}{\partial t}\right)^2 - \frac{1}{C}\left(\frac{\partial Q}{\partial x}\right)^2\right]\end{aligned} \tag{118}$$

where L is the inductance-per-unit length along the transmission line. The open ends at $x = 0$ and $x = l$ impose-boundary conditions of vanishing current. We assume the case of a nonuniform transmission line, where both C and L may depend on x. Moreover, the inductance L depends on the current I, according to (1), as a result of nonlinear kinetic inductance.

As a basis for expanding $Q(x,t)$ as

$$Q(x,t) = \sum_n q_n(t)u_n(x) \tag{119}$$

we use the solutions of

$$\frac{d}{dx}\left(\frac{1}{C}\frac{du_n}{dx}\right) = -\omega_n^2 L u_n \tag{120}$$

with the boundary conditions of vanishing current

$$u_n(0) = u_n(l) = 0. \tag{121}$$

We assume that the functions $u_n(x)$ are chosen to be real. For the case of a uniform transmission-line resonator, where both C and L are independent of x, one has $\omega_n = n\pi/l\sqrt{LC}$, where n is an integer. In the nonlinear regime, however, such an equally spaced spectrum may lead to strong intermode coupling, where harmonics and subharmonics of a driven mode excite other modes. In this paper, we assume that such intermode effects are avoided by employing a nonuniform resonator. This allows us to consider only the mode in the resonator, which is driven externally. Using the expansion of (119)

$$\begin{aligned}\mathcal{L} = \frac{1}{2}\sum_n\sum_m \dot{q}_n\dot{q}_m\int_0^l dx L_0 u_n u_m \\ -\frac{1}{2}\sum_n\sum_m q_n q_m\int_0^l dx\frac{1}{C}\frac{du_n}{dx}\frac{du_m}{dx} + \Delta\mathcal{L}\end{aligned} \tag{122}$$

where

$$\begin{aligned}\Delta\mathcal{L} = \frac{1}{2I_c^2}\sum_{n',n'',n''',n''''} \dot{q}_{n'}\dot{q}_{n''}\dot{q}_{n'''}\dot{q}_{n''''} \\ \times\int_0^l dx\, u_{n'}u_{n''}u_{n'''}u_{n''''}\Delta L.\end{aligned} \tag{123}$$

We first treat the linear part. Consider (120) for u_n multiplied by u_m and (120) for u_m multiplied by u_n

$$u_m \frac{d}{dx}\left(\frac{1}{C}\frac{du_n}{dx}\right) = -\omega_n^2 L_0 u_n u_m \tag{124}$$

$$u_n \frac{d}{dx}\left(\frac{1}{C}\frac{du_m}{dx}\right) = -\omega_m^2 L_0 u_n u_m. \tag{125}$$

Taking the difference of these two equations yields

$$\frac{d}{dx}\left(u_m \frac{1}{C}\frac{du_n}{dx} - u_n \frac{1}{C}\frac{du_m}{dx}\right) = \left(\omega_m^2 - \omega_n^2\right) L_0 u_n u_m. \tag{126}$$

Then, integrating from $x = 0$ to $x = l$, one obtains

$$\left(\omega_m^2 - \omega_n^2\right) \int_0^l dx L_0 u_n u_m = 0. \tag{127}$$

In general, it can be easily shown that the spectrum of a finite one-dimensional resonator having vanishing current-boundary conditions is nondegenerate. Thus, by requiring that the functions $u_n(x)$ are normalized, one obtains

$$\int_0^l dx L_0 u_n u_m = \delta_{nm}. \tag{128}$$

Moreover, integrating by parts and using (120) and the boundary conditions, one obtains

$$\int_0^l dx \frac{1}{C}\frac{du_n}{dx}\frac{du_m}{dx} = \omega_n^2 \int_0^l dx L_0 u_n u_m = \omega_n^2 \delta_{nm}. \tag{129}$$

Thus

$$\mathcal{L} = \frac{1}{2}\sum_n \left(\dot{q}_n^2 - \omega_n^2 q_n^2\right) + \Delta\mathcal{L}.$$

The Euler–Lagrange equation is given by

$$\frac{d}{dt}\left(\frac{\partial \mathcal{L}}{\partial \dot{q}_n}\right) - \frac{\partial \mathcal{L}}{\partial q_n} = 0. \tag{130}$$

Thus

$$\ddot{q}_n + \omega_n^2 q_n + \frac{d}{dt}\left(\frac{\partial \Delta\mathcal{L}}{\partial \dot{q}_n}\right) = 0. \tag{131}$$

The variable that is canonically conjugate to q_n is

$$p_n = \frac{\partial \mathcal{L}}{\partial \dot{q}_n} = \dot{q}_n + \frac{\partial \Delta\mathcal{L}}{\partial \dot{q}_n}. \tag{132}$$

The Hamiltonian is given by

$$\begin{aligned}\mathcal{H} &= \sum_n p_n \dot{q}_n - \mathcal{L} \\ &= \frac{1}{2}\sum_n \left[p_n^2 - \left(\frac{\partial \Delta\mathcal{L}}{\partial \dot{q}_n}\right)^2 + \omega_n^2 q_n^2\right] - \Delta\mathcal{L}.\end{aligned} \tag{133}$$

To first order in $\Delta\mathcal{L}$ (or in ΔL)

$$\mathcal{H} = \mathcal{H}_0 + \mathcal{V} \tag{134}$$

where

$$\mathcal{H}_0 = \frac{1}{2}\sum_n \left(p_n^2 + \omega_n^2 q_n^2\right) \tag{135}$$

and

$$\mathcal{V} = -\frac{1}{2I_c^2}\sum_{n',n'',n''',n''''} p_{n'} p_{n''} p_{n'''} p_{n''''} \times \int_0^l dx u_{n'} u_{n''} u_{n'''} u_{n''''} \Delta L. \tag{136}$$

In carrying out the quantization, the variables q_n and p_n are regarded as operators satisfying the following commutation relations:

$$[q_n, p_m] \equiv q_n p_m - p_m q_n = i\hbar\delta_{n,m} \tag{137}$$

$$[q_n, q_m] = [p_n, p_m] = 0. \tag{138}$$

The boson-annihilation and creation operators are defined by

$$A_n = \frac{e^{i\omega_n t}}{\sqrt{2\hbar}}\left(\sqrt{\omega_n} q_n + \frac{i}{\sqrt{\omega_n}} p_n\right) \tag{139}$$

$$A_n^\dagger = \frac{e^{-i\omega_n t}}{\sqrt{2\hbar}}\left(\sqrt{\omega_n} q_n - \frac{i}{\sqrt{\omega_n}} p_n\right). \tag{140}$$

The inverse transformation is given by

$$q_n = \sqrt{\frac{\hbar}{2\omega_n}}\left(A_n^\dagger e^{i\omega_n t} + A_n e^{-i\omega_n t}\right) \tag{141}$$

$$p_n = i\sqrt{\frac{\hbar\omega_n}{2}}\left(A_n^\dagger e^{i\omega_n t} - A_n e^{-i\omega_n t}\right). \tag{142}$$

The commutation relations for the operators A_n and $A_n^\dagger$ are derived directly from (137) and (138)

$$\left[A_n, A_m^\dagger\right] = \delta_{n,m} \tag{143}$$

$$[A_n, A_m] = \left[A_n^\dagger, A_m^\dagger\right] = 0. \tag{144}$$

Using (141) and (142), the Hamiltonian [(135)] can be expressed as

$$\mathcal{H}_0 = \sum_n \hbar\omega_n \left(A_n^\dagger A_n + \frac{1}{2}\right). \tag{145}$$

The current operator is given by

$$I(x,t) = \frac{\partial Q}{\partial t} = i\sum_n \sqrt{\frac{\hbar\omega_n}{2}}\left(A_n^\dagger e^{i\omega_n t} - A_n e^{-i\omega_n t}\right) u_n(x). \tag{146}$$

The voltage operator is given by

$$V(x,t) = -\frac{1}{C}\sum_n \sqrt{\frac{\hbar}{2\omega_n}}\left(A_n^\dagger e^{i\omega_n t} + A_n e^{-i\omega_n t}\right)\frac{du_n}{dx}. \tag{147}$$

The quantities $p_{n'}p_{n''}p_{n'''}p_{n''''}$ in general contain terms oscillating rapidly at frequencies on the order of the frequencies in the resonator spectrum. In the rotating-wave approximation (RWA), these terms are neglected, since their effect on the dynamics, on a time scale much longer compared to a typical-oscillation period, is negligibly small, and only stationary terms remain. In the expression for $\mathcal{V}$, only terms of the type $p_{n'}^2 p_{n''}^2$ contain stationary terms, which are given by

$$p_{n'}^2 p_{n''}^2 \simeq \frac{\hbar\omega_{n'}}{2}\frac{\hbar\omega_{n''}}{2}\left(1+2A_{n'}^\dagger A_{n'}\right)\left(1+2A_{n''}^\dagger A_{n''}\right). \tag{148}$$

The constant term can be disregarded, since it only gives rise to a constant phase factor. Moreover, the terms $A_{n'}^\dagger A_{n'}$ and $A_{n''}^\dagger A_{n''}$ that give rise to frequency shift can be absorbed into $\mathcal{H}_0$. Thus, in the RWA, the perturbation $\mathcal{V}$ contains only terms of the type $A_{n'}^\dagger A_{n'} A_{n''}^\dagger A_{n''}$

$$\mathcal{V} = \frac{\hbar}{2}\sum_{n'} K_{n'}\left(A_{n'}^\dagger A_{n'}\right)^2 + \hbar\sum_{n'\neq n''}\lambda_{n'n''}A_{n'}^\dagger A_{n'}A_{n''}^\dagger A_{n''} \tag{149}$$

where

$$K_{n'} = -\frac{\hbar\omega_{n'}^2}{I_c^2}\int_0^l dx\; u_{n'}^4\Delta L \tag{150}$$

and

$$\lambda_{n'n''} = -\frac{3\hbar\omega_{n'}\omega_{n''}}{I_c^2}\int_0^l dx u_{n'}^2 u_{n''}^2\Delta L. \tag{151}$$

The effect of the nonlinear-intermode coupling terms in (149), which is disregarded in this paper, is studied in [35].

Appendix B
Nonlinear Losses Associated With the Kinetic Inductance

Here, we derive expressions for the linear and nonlinear loss coefficients γ_2 and γ_3 in terms of the parameters that characterize the resistive loss associated with the kinetic inductance. This is accomplished by obtaining an expression for the rate-of-energy loss in the cavity in terms of the model parameters and comparing it with the expression for the power dissipated due to the resistance associated with the kinetic inductance. The equation of motion for the resonator Hamiltonian H_r [(3)]

$$i\hbar\frac{dH_r}{dt} = [H_r, H] \tag{152}$$

yields

$$\begin{aligned}\frac{dH_r}{dt} =& -i\hbar\omega_0\int d\omega\left[\kappa_1 A^\dagger a_1(\omega) - \kappa_1^* a_1^\dagger(\omega)A\right]\\ &- i\hbar\omega_0\int d\omega\left[\kappa_2 A^\dagger a_2(\omega) - \kappa_2^* a_2^\dagger(\omega)A\right]\\ &- 2i\hbar\omega_0\int d\omega\left[\kappa_3 A^\dagger A^\dagger a_3(\omega) - \kappa_3^* a_3^\dagger(\omega)AA\right]\\ &- 2i\hbar K\int d\omega\left[\kappa_3 A^\dagger A^\dagger a_3(\omega) - \kappa_3^* a_3^\dagger(\omega)AA\right]\\ &- i\hbar K\int d\omega\left[\kappa_1 A^\dagger A^\dagger A a_1(\omega) - \kappa_1^* a_1^\dagger(\omega)A^\dagger AA\right]\\ &- i\hbar K\int d\omega\left[\kappa_2 A^\dagger A^\dagger A a_2(\omega) - \kappa_2^* a_2^\dagger(\omega)A^\dagger AA\right]\\ &- 2i\hbar K\int d\omega\left[\kappa_3 A^\dagger A^\dagger A^\dagger A a_3(\omega) - \kappa_3^* a_3^\dagger(\omega)A^\dagger AAA\right].\end{aligned} \tag{153}$$

As was shown by Gardiner and Collett [21], [22], the equations of motion (16)–(18) for the baths can be integrated to yield

$$\frac{1}{\sqrt{2\pi}}\int d\omega\; a_1(\omega) = a_1^{\rm in}(t) - i\sqrt{\frac{\pi}{2}}\kappa_1^* A(t). \tag{154}$$

Similarly

$$\frac{1}{\sqrt{2\pi}}\int d\omega\; a_2(\omega) = a_2^{\rm in}(t) - i\sqrt{\frac{\pi}{2}}\kappa_2^* A(t) \tag{155}$$

and

$$\frac{1}{\sqrt{2\pi}}\int d\omega\; a_3(\omega) = a_3^{\rm in}(t) - i\sqrt{\frac{\pi}{2}}\kappa_3^* A(t)A(t). \tag{156}$$

These expressions can be used to eliminate the $a_n(\omega)$ from (153). Evaluating the expectation value of (153) with respect to a state in which all the bath modes are in a vacuum state, that is

$$a_n^{\rm in}(t)|0\rangle = 0 \tag{157}$$

one obtains

$$\begin{aligned}\left\langle\frac{dH_r}{dt}\right\rangle =& -2\hbar\omega_0\left[\gamma_1\langle A^\dagger A\rangle + \gamma_2\langle A^\dagger A\rangle + 2\gamma_3\langle A^\dagger A^\dagger AA\rangle\right]\\ &- 2\hbar K\left[\gamma_1\langle A^\dagger A^\dagger AA\rangle + \gamma_2\langle A^\dagger A^\dagger AA\rangle\right.\\ &\left.+ 2\gamma_3\langle A^\dagger A^\dagger AA\rangle + 2\gamma_3\langle A^\dagger A^\dagger A^\dagger AAA\rangle\right].\end{aligned} \tag{158}$$

If $\omega_0 \gg K$, then as long as the mean-field is not too large, one has, to a good approximation

$$\left\langle\frac{dH_r}{dt}\right\rangle = -2\hbar\omega_0\left[\gamma_1\langle A^\dagger A\rangle + \gamma_2\langle A^\dagger A\rangle + 2\gamma_3\langle A^\dagger A^\dagger AA\rangle\right]. \tag{159}$$

This is an expression for the rate with which energy is lost from the cavity.

The power dissipated within the cavity is given by

$$P = \int_0^L dx \, \langle : RI^2 : \rangle \tag{160}$$

where the ": :" denotes normal ordering. Using (2), this can be written as

$$P = \int_0^l dx \, R_0 \langle : I^2 : \rangle + \frac{1}{I_c^2} \int_0^l dx \Delta R \langle : I^4 : \rangle \tag{161}$$

where we have allowed for the possibility that R_0 and ΔR may be functions of the distance x along the resonator, as would be the expected case if the composition and shape of the transmission-line cross section varies with x. Substituting (146) into this equation yields

$$P = \hbar\omega_n \int_0^l dx \, R_0 u_n^2 \left\langle A_n^\dagger A_n \right\rangle + \frac{3(\hbar\omega_n)^2}{2I_c^2} \int_0^l dx \, u_n^4 \Delta R \left\langle A_n^\dagger A_n^\dagger A_n A_n \right\rangle. \tag{162}$$

In order to make the comparison of this equation with that of (159), we consider the unloaded cavity case when the coupling through the signal port of the cavity is set to zero, that is

$$\gamma_1 = 0. \tag{163}$$

Setting

$$P = -\left\langle \frac{dH_r}{dt} \right\rangle \tag{164}$$

and keeping in mind that, presently, ω_0 and ω_n both denote the resonance frequency of the same selected mode, one has

$$\gamma_2 = \frac{1}{2} \int_0^l dx \, u_n^2 R_0 \tag{165}$$

and

$$\gamma_3 = \frac{3\hbar\omega_0}{8I_c^2} \int_0^l dx \, u_n^4 \Delta R. \tag{166}$$

REFERENCES

[1] J. R. Tucker, "Quantum limited detection in tunnel junction mixers," *IEEE J. Quantum Electron.*, vol. QE-15, no. 11, pp. 1234–1258, Nov. 1979.

[2] J. R. Tucker and M. J. Feldman, "Quantum detection at millimeter wavelengths," *Rev. Mod. Phys.*, vol. 57, no. 4, pp. 1055–1113, 1985.

[3] L. S. Kuzmin, K. K. Likharev, V. V. Migulin, and A. B. Zorin, "Quantum noise in Josephson-junction parametric amplifiers," *IEEE Trans. Magn.*, vol. MAG-19, no. 3, pp. 618–621, May 1983.

[4] B. Yurke, L. R. Corruccini, P. G. Kaminsky, L. W. Rupp, A. D. Smith, A. H. Silver, R. W. Simon, and E. A. Whittaker, "Observation of parametric amplification and deamplification in a Josephson parametric amplifier," *Phys. Rev. A, Gen. Phys.*, vol. 39, no. 5, pp. 2519–2533, Mar. 1989.

[5] R. Movshovich, B. Yurke, P. G. Kaminsky, A. D. Smith, A. H. Silver, R. W. Simon, and M. V. Schneider, "Observation of zero-point noise squeezing via a Josephson-parametric amplifier," *Phys. Rev. Lett.*, vol. 65, no. 12, pp. 1419–1422, Sep. 1990.

[6] T. Dahm and D. J. Scalapino, "Theory of intermodulation in a superconducting microstrip resonator," *J. Appl. Phys.*, vol. 81, no. 4, pp. 2002–2009, Feb. 1997.

[7] B. Abdo, E. Segev, O. Shtempluck, and E. Buks, "Observation of bifurcations and hysteresis in nonlinear NbN superconducting microwave resonators," *IEEE Trans. Appl. Superconduc.*, no. 99, Jan. 10, 2005. Digital Object Identifier: 10.1109/TASC.2006.881823.

[8] ——, "Nonlinear dynamics in the resonance lineshape of NbN superconducting resonators," *Phys. Rev. B, Condens. Matter*, vol. 73, no. 13, p. 134 513, Jan. 8, 2006.

[9] ——, "Intermodulation gain in nonlinear NbN superconducting microwave resonators," *Appl. Phys. Lett.*, vol. 88, no. 2, pp. 022508 1–022508 3, 2006.

[10] ——, *Nonlinear Coupling in Nb/NbN Superconducting Microwave Resonators*, Jan. 11, 2005. arXiv:cond-mat/0501236.

[11] A. Villeneuve, C. C. Yang, G. I. Stegeman, C.-H. Lin, and H.-H. Lin, "Nonlinear refractive-index and two photon-absorption near half the band gap in AlGaAs," *Appl. Phys. Lett.*, vol. 62, no. 20, pp. 2465–2467, May 1993.

[12] A. M. Fox, J. J. Baumberg, M. Dabbicco, B. Huttner, and J. F. Ryan, "Squeezed light generation in semiconductors," *Phys. Rev. Lett.*, vol. 74, no. 10, pp. 1728–1731, Mar. 1995.

[13] S.-T. Ho, X. Zhang, and M. K. Udo, "Single-beam squeezed-state generation in semiconductor waveguides with $\chi^{(3)}$ nonlinearity at below half-band gap," *J. Opt. Soc. Amer. B, Opt. Phys.*, vol. 12, no. 9, pp. 1537–1549, Sep. 1995.

[14] S. Zaitsev, R. Almog, O. Shtempluck, and E. Buks, *Nonlinear Damping in Nanomechanical Beam Oscillator*, Mar. 6, 2005. arXiv:cond-mat/053130v1.

[15] R. Almog, S. Zaitsev, O. Shtempluck, and E. Buks, "High intermodulation gain in a micromechanical duffing resonator," *Appl. Phys. Lett.*, vol. 88, no. 21, p. 213 509, 2006.

[16] ——, *Noise Squeezing in a Nanomechanical Duffing Resonator*, Jul. 6, 2006. arXiv:cond-mat/0607055.

[17] E. Buks and B. Yurke, "Mass detection with nonlinear nanomechanical resonator," *Phys. Rev. E, Stat. Phys. Plasmas Fluids Relat. Interdiscip. Top.*, vol. 74, no. 4, p. 046 619, Jul. 5, 2006.

[18] C. C. Gerrry and E. E. Hach, III, "Enhanced squeezing from a Kerr medium combined with two-photon absorption," *Opt. Commun.*, vol. 100, no. 1–4, pp. 211–214, Jul. 1993.

[19] L. Gilles, B. M. Garraway, and P. L. Knight, "Generation of nonclassical light by dissipative two-photon processes," *Phys. Rev. A, Gen. Phys.*, vol. 49, no. 4, pp. 2785–2799, Apr. 1994.

[20] G. X. Li, J. S. Peng, and P. Zhou, "Squeezing of field in the system of a Kerr medium embedded in a nondegenerate two-photon absorption cavity," *Chin. Phys. Lett.*, vol. 12, no. 2, pp. 79–82, 1995.

[21] C. W. Gardiner and M. J. Collett, "Input and output in damped quantum systems: Quantum stochastic differential equations and the master equation," *Phys. Rev. A, Gen. Phys.*, vol. 31, no. 6, pp. 3761–3774, Jun. 1985.

[22] J. Gea-Banacloche, N. Lu, L. M. Pedrotti, S. Prasad, M. O. Scully, and K. Wodkiewich, "Treatment of the spectrum of squeezing based on the modes of the Universe. I. Theory and a physical picture," *Phys. Rev. A, Gen. Phys.*, vol. 41, no. 1, pp. 369–380, Jan. 1990.

[23] N. Imoto, H. A. Haus, and Y. Yamamoto, "Quantum nondemolition measurement of the photon number via the optical Kerr effect," *Phys. Rev. A, Gen. Phys.*, vol. 32, no. 4, pp. 2287–2292, Oct. 1985.

[24] A. G. White, P. K. Lam, D. E. McClelland, H.-A. Bachor, and J. Munro, "Kerr noise reduction and squeezing," *J. Opt., B Quantum Semiclass. Opt.*, vol. 2, no. 4, pp. 553–561, 2000.

[25] B. Yurke and J. S. Denker, "Quantum network theory," *Phys. Rev. A, Gen. Phys.*, vol. 29, no. 3, pp. 1419–1437, Mar. 1984.

[26] N. Tornau and A. Bach, "Quantum statistics of two-photon absorption," *Opt. Commun.*, vol. 11, no. 1, pp. 46–49, May 1974.

[27] G. S. Agarwal and G. P. Hildred, "Time development of squeezing in two photon absorption," *Opt. Commun.*, vol. 58, no. 4, pp. 287–289, Jun. 1986.

[28] L. Gilles and P. L. Knight, "Two-photon absorption and nonclassical states of light," *Phys. Rev. A, Gen. Phys.*, vol. 48, no. 2, pp. 1582–1593, Aug. 1993.

[29] H. Ezaki, "Photon number squeezing due to two-photon absorption in internal and external fields of a microcavity," *J. Phys. Soc. Jpn.*, vol. 68, no. 5, pp. 1562–1566, May 1999.

[30] M. Kitamura and T. Tokihiro, "Squeezed states of light in a cavity with a local two-photon absorber," *J. Opt., B Quantum Semiclass. Opt.*, vol. 1, no. 5, pp. 546–556, Oct. 1999.
[31] A. H. Nayfeh and D. T. Mook, *Nonlinear Oscillations*. Hoboken, NJ: Wiley, 1979.
[32] L. D. Landau, *Mechanics*, 3rd ed. New York: Pergamon, 1976.
[33] B. Yurke, D. S. Greywall, A. N. Pargellis, and P. A. Busch, "Theory of amplifier-noise evasion in an oscillator employing a nonlinear resonator," *Phys. Rev. A, Gen. Phys.*, vol. 51, no. 5, pp. 4211–4229, May 1995.
[34] B. Yurke, "Squeezed-coherent-state generation via four-wave mixers and detection via homodyne detectors," *Phys. Rev. A, Gen. Phys.*, vol. 32, no. 1, pp. 300–310, Jul. 1985.
[35] E. Buks and B. Yurke, "Dephasing due to intermode coupling in superconducting stripline resonators," *Phys. Rev. A, Gen. Phys.*, vol. 73, no. 2, p. 023 815, 2006.

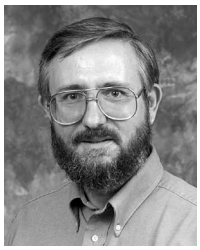

Bernard Yurke received the B.S. and M.A. degrees in physics from the University of Texas at Austin. He received the Ph.D. form Cornell University, Ithaca, NY, for experimental work in low-temperature physics, in 1982.

He has since been a Research Physicist at Bell Laboratories, Lucent Technologies, Murray Hill, NJ. He has worked in variety of fields including quantum optics, condensed matter, biophysics, and microelectromechanical systems. His current research interests include DNA-based nanodevices and materials.

Dr. Yurke is a distinguished member of Technical Staff at Bell Laboratories, as well as a fellow of the Optical Society of America, the American Physical Society, and the American Association for the Advancement of Science. He received a Max Born Award from the Optical Society of America for his work in quantum optics.

Eyal Buks received the B.Sc. degree in mathematics and physics from the Tel-Aviv University, Tel-Aviv, Israel, in 1991, and the M.Sc. and Ph.D. degrees in physics from the Weizmann Institute of Science, Rehovat, Israel, in 1994, and 1998, respectively. His graduate work concentrated on interference and dephasing in mesoscopic systems.

From 1998 to 2002, he worked at the California Institute of Technology, Pasadena, as a Postdoctoral Scholar, studying experimentally nanomachining devices. He is currently a Senior Lecturer at the Technion–Israel Institute of Technology, Haifa, Israel. His current research is focused on nanomachining and mesoscopic physics.